**THERMALLY DRIVEN FORMATION OF FRACTURES ON COMET 67P/CHURYUMOV-GERASIMENKO.** J. L. Molaro[1], P. Becerra[2], C. Herny[2], R. Marschall[2], M.R. El-Maarry[3], N. Thomas[2], A. Pommerol[2], and P. Theologou[2]. [1]Planetary Science Institute (jmolaro@psi.edu), [2]Physikalisches Institut, Universität Bern, Switzerland, [3]Laboratory for Atmospheric and Space Physics, University of Colorado.

**Introduction:** The Optical, Spectroscopic, and Infrared Remote Imaging System (OSIRIS) [1] on board ESA's Rosetta spacecraft observed many fractures on the surface of comet 67P/Churyumov-Gerasimenko [2]. These appear over many morphological regions at scales from sub-meter (Fig. 1) to 10s of meters (Fig. 2) and larger, and were initially assessed and classified by [3] based on their morphology and possible formation mechanisms. Evidence suggests that fracturing of solid material on the comet contributes to the development of unconsolidated regolith and boulders [4], and thus investigating these formation mechanisms will provide insight into both its recent history and long-term landscape evolution.

The most likely mechanism responsible for developing small scale fractures is thermally induced crack propagation, which is thought to operate on a variety of airless bodies [e.g., 5-8] to cause rock breakdown, crater degredation, and regolith production. Recent modeling work [5] has shown that spatially and temporally varying stress fields are induced in boulders undergoing diurnal thermal cycling on the Moon, which drive crack propagation in different directions and at different locations within their volume. Similar stresses may drive the development of fractures in meter scale boulders on comet 67P (Figure 1b), though their locations (and thus the nature of breakdown) may differ on the two surfaces. The comet also undergoes a seasonal thermal cycle over its ~6 year orbit, which will induce stress fields at the 10s of meter scale, which may drive crack propagation in large topographic features such as exposed cliff faces (Figure 1, c).

While propagation rates and stress thresholds are not well constrained, pairing such models with OSIRIS images of fractures on comet 67P provides an unparalleled opportunity to study this process. We will characterize and compare OSIRIS images of fractures before and after perihelion passage, and model the macroscopic stresses induced in the associated topographic features along the comet's orbital path. By relating the simulated stress fields to observed features on the comet's surface, we can assess whether or not those features were thermally driven, explore how they develop over time, and constrain stress thresholds and propagation rates on the comet.

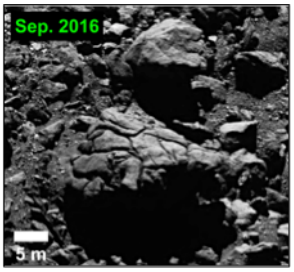


Figure 1. Boulders observed in the Nut region. The larger boulder exhibits substantial fracturing, while the smaller boulders appear consolidated and relatively fracture-free.

**Model:** Following the work of [5], we use COMSOL Multiphysics to perform 3D finite element simulations of the thermomechanical response of boulders and cliff faces on the surface of the comet to diurnal and seasonal thermal cycling. This allows us to investigate the magnitude and distribution of the resulting stresses. We model a spherical boulder embedded in a volume of regolith, impose incident solar radiation on the surface and solve the heat and displacement equations over several solar days as the comet passes through perihelion. The model accounts for topographic shadowing, radiative and conductive interaction between the boulder and surrounding regolith, as well as the size of the solar disk. We approximate the regolith as lunar regolith, with temperature and depth dependent material properties following [9], producing a temperature range and thermal inertia that are consistent with measurements taken by the MIRO instrument aboard Rosetta [10]. The boulder is composed of a mixture of basalt and 25% water ice by volume, which also have temperature dependent properties [5, 8]. We also model a stepped, vertical cliff face with the same composition. The horizontal surfaces are thermally insulated (as if regolith covered), except for a stripe at the cliff's edge where some observations show exposed rock. The model setup for this simulation is the same as for the boulder, except that the edges and

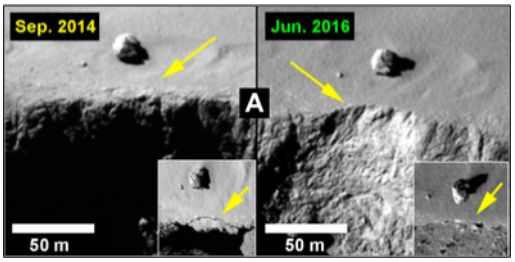


Figure 2. Observed cliff collapse (yellow arrows) at Aswan cliff in the region of Seth, as approximated by our idealized cliff model.

base of the cliff are spatially fixed and it is solved over a period of ~2 years or ~1/3 of its orbit.

**Preliminary Results:** For a 1 m boulder, peak diurnal stresses occur during late afternoon (Fig. 3). Unlike in lunar boulders [5], these peak stresses occur in the interior, suggesting that the primary mode of thermal breakdown is the development of through-going cracks (Fig. 1) rather than disaggregation of the near-surface. These stresses reach a maximum magnitude of ~7 MPa at perihelion when the boulder has the greatest diurnal temperature range. There is a complex relationship between boulder size and rotation period that determines where and when peak stresses occur. Future work will explore this relationship on 67P/ G-C in more detail. Additionally, the boulder's temperature ranges from 251-277 K, suggesting that sublimation effects within pores may produce additional stresses that interact with the thermally induced stress field.

Peak seasonal stresses on the cliff face occur after perihelion as it begins to cool, and reach a maximum of ~20 MPa (Fig. 4). These stresses are oriented vertically, parallel to the cliff face, and drive edge-parallel crack propagation. There are many observations of such edge-parallel cracks found on the comet, such as shown in Fig. 2. Similarly, the horizontal cliff top will also develop edge-parallel cracks if it has regolith cover thinner than the seasonal skin depth (~2 m), as observed in some images (Fig. 3). If regolith cover extends to the cliff edge, the horizontal cliff top is insulated from strong thermal stresses, but the stress field at the cliff interior and vertical face remain unchanged.

**Conclusions and Future Work:** These simulations demonstrate that stress fields generated by diurnal and seasonal thermal cycles are consistent with certain features observed on the surface of comet 67P/G-C, such as through-going fractures in rocks (Fig. 1). Our results suggest that the rockfall observed at Aswan Cliff during the Rosetta mission (Fig. 2) may have been thermomechanically driven, providing the first constraint on the stress threshold (~20 MPa) required to generate such activity on cometary surfaces. Realistically, the size and shape of topographic features, as well as pre-existing damage, will influence the magnitude and nature of induced stress fields and the direction of crack propagation. However, such an order of magnitude stress threshold is useful for comparing the stress fields of different features, or determining the relative efficacy of this process between bodies. In future work, we will locate additional observations of cracks, rock falls, or other features that occurred on comet 67P/G-C during Rosetta's mission lifetime. We will use the shape model to simulate these real topographical features on and explore the role this process plays in the evolution of its surface.

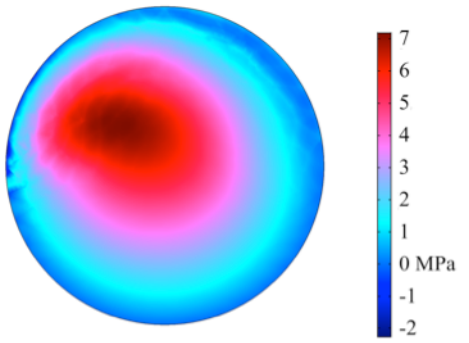


Figure 3. Snapshot of the state of peak stress in a 2D cross section through a 1 m diameter boulder, which occurs during late afternoon. The parameter shown is the maximum principal stress (where tensile stress is positive), which represents the most amount of idealized energy available for crack propagation at a given location.

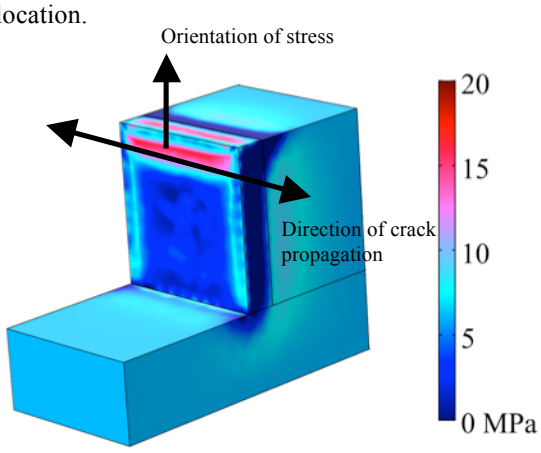


Figure 4. Snapshot of the state of peak stress 100 m in a vertical cliff face, which occurs just after perihelion.

**References:** [1] Keller, H. U. et al. *Space Sci. Rev. 128, 433–506* (2007). [2] Thomas, N. et al. *Science 347,* (2015). [3] El-Maarry, M. R. et al. *Geophys. Res. Lett. 42, 5170–5178* (2015). [4] El-Maarry, M.R. et al. *Science*, (2017). [5] Molaro J.L. et al. *Icarus* (2017). [6] Molaro J. L. et al. *J. of Geophys. Res. 120,* 255-277 (2015). [7] Jewitt D. and J. Li *The Astr. Journal, 140,* 1519 (2010). [8] Molaro, J.L and C.B. Phillips, *LPSC XLVIII, Abs. 1729* (2017). [9] Vasavada, A.R. et al. *Geoph. Res. Lett., 117,* E00H18 (2012). [10] Gulkis, S. et al. *Science 347,* 6220 (2015).

**Acknowledgements:** This project has also received funding from the European Union's Horizon 2020 research and innovation programme under grant agreement Nº 686709 and was also supported by the Swiss State Secretariat for Education, Research and Innovation (SERI) under contract number 16.0008-2.